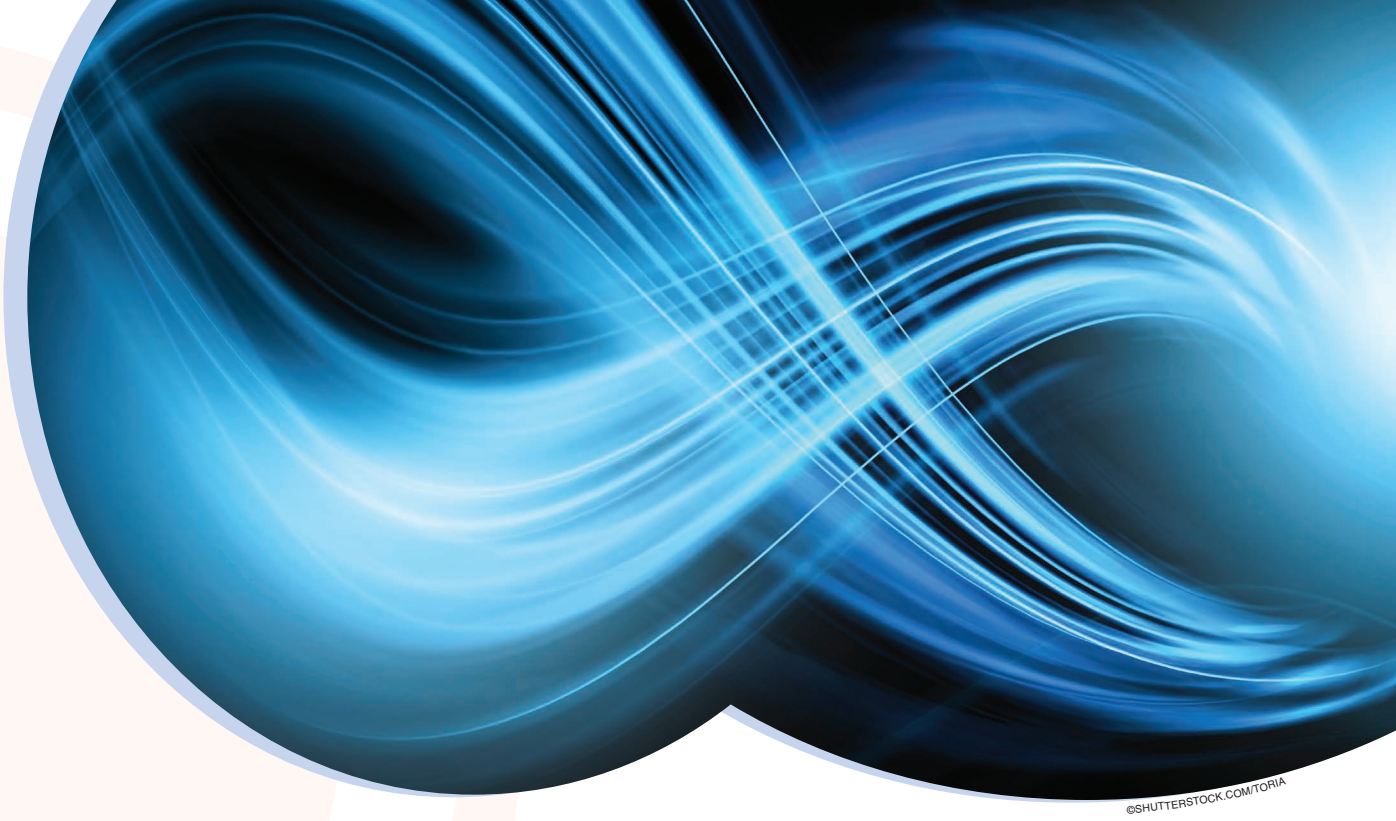

Ovidio Mario Bucci and Marco Donald Migliore

Degrees of Freedom and Sampling Representation of Electromagnetic Fields

Concepts and applications.

This article reviews the development of the concept of the number of degrees of freedom (DOF), or NDF, of radiated or scattered fields and of optimized sampling expansions for their adequate representation, highlighting their impact on the amount of information that a communication system exploiting electromagnetic fields can transmit. After summarizing and discussing the concept of DOF and its relationship with the mathematical properties of the radiated fields, the concept of spatial bandwidth of the electromagnetic field is reviewed. Then, the approximation of the field using band-limited functions is discussed, clarifying the convenience of sampling representations and including a new analysis of their redundancy with respect to the NDF. Finally, we provide an updated overview of their application in many fields of practical

Digital Object Identifier 10.1109/MAP.2024.3513216
Date of publication 30 December 2024; date of current version 18 June 2025

interest, both in classical areas of applied electromagnetics and in the emerging electromagnetic information theory sector.

INTRODUCTION

The ability to describe the incredible complexity of electromagnetic phenomena through fields governed by just four equations is one of the most profound achievements of physics and a pillar of modern technology. However, when passing from mathematics to the real world, as we can perform only a finite number of approximate measurements or numerical evaluations, it is clear (even if scarcely emphasized) that we can never determine a field, which is a function, unless some a priori information and the constraints that Maxwell's equations impose on the field allow its representation (within a given precision) in terms of a finite number of parameters.

Among all possible representations, linear ones are particularly relevant as they allow linear algebra and analysis and highly efficient numerical implementations on modern computers. Hence, identifying the minimum number of parameters that allows for a linear representation of the field is a problem of great theoretical and applicative relevance. As the number of parameters describing the state of a physical system is called its *NDF*, it is natural to identify such a number with the NDF of the field.

Exploiting the band-limiting characteristics of optical systems and the cardinal sampling series [1], Toraldo di Francia [2] defined the NDF of an optical image, and Landau and Pollak rigorously assessed the concept a few years later [3].

Extending these results to nonoptical frequencies and applications is by no means straightforward as the Fourier transform relationship between source and field and the field bandlimitedness are usually lost. Accordingly, the definition of the NDF must be revised, and adopting a sampling representation requires deep analysis to establish to what extent and how band-limited functions can approximate electromagnetic fields.

Thus, a satisfactory answer to these questions, first provided by Bucci and his coworkers during the 1980s and the 1990s [4], [5], [6], is the preliminary condition for the general solution of the problem of an efficient and accurate representation of radiated fields, given a desired precision level. However, representing the field is only one face of the medal. Considering that fields mathematically distinct but differing less than the precision limits dictated by the noise level, measurement accuracy, resolution, etc., must be considered indistinguishable as physical entities, we are naturally led to inquire as to what is the maximum number of distinguishable fields that a source of bounded extension and intensity can radiate.

This is a crucial point as the amount of information that a communication system exploiting electromagnetic fields can transmit depends on the number of spatial configurations of the field that can be generated per unit of time and are distinguishable by the receivers. Hence, the support of the information is no longer a logical and abstract quantity (a string of bits) but becomes a physical object [7]. The logarithm of the maximum number of distinguishable fields in the presence of a level ϵ of uncertainty is called the ϵ-capacity of the set of fields radiated by the source [8] and is analogous to the channel capacity, while the NDF at the level ϵ is strictly related to the maximum number of spatial subchannels that can be used in multiple-input, multiple-output (MIMO) communication systems [9].

This article summarizes the theory that allows us to deal with the two faces of the medal in a unitary and coherent way, by following the path that led to a general, rigorous definition of the NDF of radiated or scattered fields and to the development of optimized sampling expansions for their effective representation. That information then provided a connection between information and electromagnetism [10] and led to the birth of a new discipline, called *electromagnetic information theory* (*EIT*) [11], [12], which involves both the electromagnetic and communication communities.

We also present some new results and an updated account of the application of the theory to a vast set of different practical problems.

The next section summarizes and discusses the concept of DOF and its relationship with the mathematical properties of the radiated fields, showing the practical convenience of sampling representations compared to the "optimal" ones, i.e., those involving the minimum number of parameters. This naturally leads to the concept of the effective bandwidth of electromagnetic fields and the corresponding sampling representations, summarized and discussed in the section "Effective Field Bandwidth and Sampling Representation." In the same section, we also present a new analysis of the factors affecting the redundancy of sampling representations. The section "Applications" presents an updated summary of the exploitations of the previous results in several application sectors, both in classical areas of applied electromagnetics and in EIT. Conclusions follow in the final section.

DOF OF THE ELECTROMAGNETIC FIELD

Let us consider a generic radiation model, consisting of an arbitrary harmonic electromagnetic source in free space, placed inside a limited volume D, bounded by a regular surface Ξ (see Figure 1) and a bounded observation surface Σ, external to D.

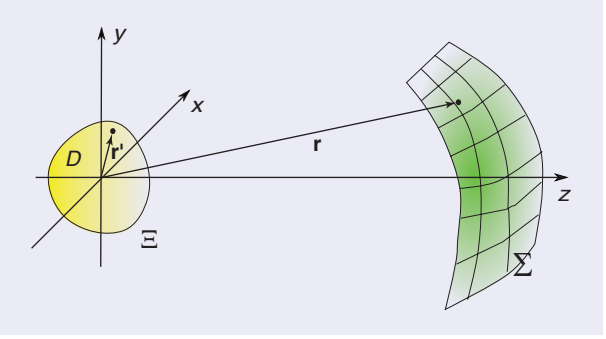

FIGURE 1. The geometry of the problem. D: electromagnetic source domain bounded by the surface Ξ; Σ: observation surface; $\mathbf{r}'$ and $\mathbf{r}$ are, respectively, the vector coordinates of the current and observation points.

For the sake of notational simplicity, as a first step we will analyze the scalar case.

In the phasor representation, the field E radiated on the surface Σ is given by [13]

$$E(\mathbf{r}) = \int_D G(\mathbf{r}, \mathbf{r}')J(\mathbf{r}')d\mathbf{r}' \tag{1}$$

where $\mathbf{r} \in \Sigma, \mathbf{r}' \in D$, G is the Green function, and J is the source current density. As any physical source is of finite energy, it is understood that J and, consequently, E are square integrable functions, and the standard L^2-norm in the corresponding Hilbert spaces is considered in the following.

In any practical instance, the source's energy is bounded. Accordingly, without loss of generality, we impose $\|J\| \leq 1, \|\cdot\|$ denoting the L^2-norm. Hence, the set X of all possible current distributions in D is the unit ball in the corresponding Hilbert space.

The set Y of the field distributions on Σ radiated by the elements of X is provided by (1), which can be rewritten in an operator form as

$$y = \mathcal{A}x \tag{2}$$

where $x \in X$ and $y \in Y$, and $\mathcal{A}: x \in X \rightarrow y \in Y$ is the radiation operator, namely the integral operator in (1), which maps the elements of X into Y (see Figure 2). As integral operators are linear and continuous, $\mathcal{A}$ is bounded; namely, it maps bounded sets into bounded sets, so that Y is bounded. In the following, we assume that $\sup_{y\in Y}(\|y\|) = \sup_{x\in X}(\|Ax\|) = 1$, which amounts to a proper scaling of the Green function. Hence, being the image of a ball through a linear mapping, Y is a hyperellipsoid, with the largest semiaxis equal to 1. Moreover, because its kernel is continuous in both its variables (indeed analytic), as Σ is external to D, the radiation operator is not only bounded but also compact (also called *completely continuous*) [14]. This means that the radiation operator transforms bounded sets into precompact sets, i.e., sets whose closure is compact. Hence, the (closure of) set Y is a compact hyperellipsoid. This implies that the semiaxes of the hyperellipsoid constitute a nonincreasing sequence converging to zero. Otherwise, it would include a closed ball of radius larger than zero, which is not compact in an infinite-dimensional space.

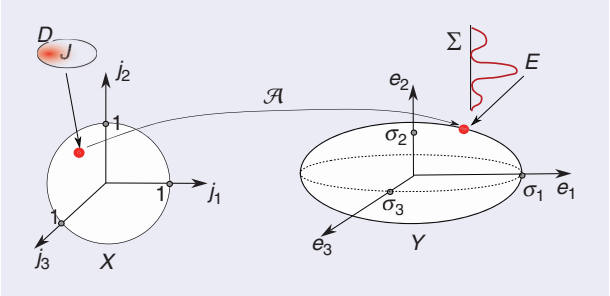

FIGURE 2. The radiation model. X is the set of the current distributions in D, and Y is the set of radiated fields on Σ; operator $\mathcal{A}$ maps the current distributions in the field distribution on the observation domain Σ.

It follows that Y is an "almost" finite-dimensional set, in the sense that it is possible to approximate all of the elements of the set with elements of a *finite-dimensional subspace* with an arbitrarily small error.

For a generic n-dimensional subspace, say L_n, the extremum of the error in approximating the elements of Y with those of L_n is equal to

$$\delta(Y, L_n) = \sup_{y\in Y}\left(\inf_{z\in L_n}\|y - z\|\right) \tag{3}$$

which is called the separation (or deviation) of Y from L_n [15]. Of course, the best choice for L_n is that minimizing the corresponding separation and thus providing the minimum approximation error achievable with an n-dimensional subspace. The separation, δ_n, of Y from such an optimal subspace is called the (Kolmogorov) n-width of Y [15].

Conversely, the minimum dimension needed to ensure an error not larger than a given value, say ϵ, is

$$n(\varepsilon) = \inf\{n : \delta_n \leq \varepsilon\}. \tag{4}$$

In our case, Y being a hyperellipsoid, δ_n has a very simple geometrical interpretation: it is just the "length" of the $(n+1)$th axis of the hyperellipsoid. Accordingly, the optimal orthonormal basis for representing the elements of Y is provided by unit vectors directed along the axes of the hyperellipsoid.[1]

The optimal basis $\{e_1, e_2 \ldots e_n, \ldots\}$ and the n-widths can be determined by exploiting the Hilbert–Schmidt decomposition[2] of the radiation operator:

$$\mathcal{A}(\cdot) = \sum_{n=1}^{\infty} \sigma_n e_n \langle j_n | \cdot \rangle \tag{5}$$

where σ_n is the nth singular value (in order of nonincreasing magnitude), e_n and j_n are the corresponding left and right singular functions, respectively, and $\langle \cdot \rangle$ stands for the inner product in L^2. Note explicitly that $\sigma_1 = 1, \sigma_{n+1} = \delta_n$, and that the right singular functions provide an orthonormal basis for the space of the radiating sources.

The reported results entail that, given the precision limit as quantified by the overall error ϵ, the radiated field can be represented in terms of a minimal number of parameters (namely, its "coordinates" in an optimal basis) equal to $n(\epsilon)$, which can be identified with the NDF of the radiated field at the level ϵ, say NDF_ϵ [5], [16]. Of course, NDF_ϵ also provides the effective rank of the radiation operator, which can be substituted with the corresponding truncated version of its Hilbert–Schmidt expansion (5).

As $n(\varepsilon) = \inf\{n : \sigma_{n+1} \leq \varepsilon\}$, the behavior of NDF_ϵ is dictated by that of the singular values of the radiation operator, which depends on the properties of its kernel, which, as previously noted, is an analytic function. Provided that the observation

[1]Of course, should some axes have equal length, the optimal basis is not unique.

[2]The Hilbert–Schmidt decomposition is the generalization to compact operators in infinite-dimensional space of the well-known singular value decomposition (SVD) of matrices.

domain is also an analytic manifold, $\mathcal{A}\mathcal{A}^{\dagger}$ ($A^{\dagger}$ denoting the adjoint), whose eigenvalues are equal to σ_n^2, is a definite positive self-adjoint operator with an analytic kernel. This implies [17], [18] that σ_n^2, and hence σ_n, will go to zero as n goes to infinity more rapidly than any power.

For example, Figure 3 shows the normalized singular values of the radiation operator of a semispherical source of radius equal to five wavelengths, relative to meridian and equatorial circumferences, of radius equal to eight wavelengths and in the far field, respectively. As can be seen, the singular values exhibit a step-like behavior: a gentle decrease up to a critical value of the index, followed by the expected sharp drop. Moreover, after the knee, the variation of $n(\epsilon)$ as we move from the near to the far field is negligible up to values of ϵ less than –100 dB. As shown in [5], this behavior is related to the quasi (spatial) band limitation of the radiated fields (to be discussed in the section "Effective Field Bandwidth and Sampling Representation") and is quite general. In the high-frequency limit, it stays valid for arbitrary analytical observation curves, so long as their separation from the source exceeds a small fraction of the source size. Therefore, $NDF\epsilon$ is *scarcely dependent* on ϵ and *slightly larger* than the critical index for (electrically) large sources and reasonable error levels.

The preceding theory has been outlined in the case of a scalar field for the sake of simplicity. The extension to vector fields is relatively straightforward; we substitute the scalar fields with the corresponding vectorial ones and the Green function with the Green dyadic, operating component-wise. Specifically, by the uniqueness theorem, the tangential field components on a closed surface surrounding the source uniquely determine the external field; thus, it follows that the NDF of the field at the exterior of any surface separated from a large source by a small fraction of the source size is slightly larger than twice the critical index.

From a mathematical point of view, the theory provides a complete answer to the problem of representing the field with a minimum number of elements of information. However, such an answer can be far from satisfactory from a practical point of view.

To be useful, a representation should satisfy two requirements. First, the elements of information should be efficiently evaluable from the source (in the case of radiated field evaluation) or measurements performed in the domain Σ of interest (in the case of field measurements). Second, the values of the field in Σ should be efficiently computable from the information elements.

Let us analyze this point, leaving aside the computational and storage burden of computing the singular values and the singular functions. In the case of field evaluation, the burden required to compute an element of information, namely the inner product in (5), is equal to that of evaluating a field sample from the source exploiting (1). By contrast, the cost of evaluating a field sample from the elements of information is proportional to NDF_ϵ. Conversely, to evaluate a field sample from field measurements, we must first perform NDF_ϵ inner products to compute the elements of information, namely the components of the field in the basis $e_1, e_2, \ldots, e_{NDF_\epsilon}$. This computation requires a number of measured field values larger (possibly significantly larger) than NDF_ϵ with a corresponding increase of the computational burden.

Hence, a representation adopting as elements of information field samples, in number not too much larger than NDF_ϵ but allowing one to recover the field inside Σ from small subsets of such samples, would be more effective than that exploiting the Hilbert–Schmidt decomposition, particularly in the case of field measurements.

Now, sampling representations, whose prototype is the classical cardinal series [1], are the standard tool adopted in signal analysis and as such have been the subject of long and exhaustive study and development. They not only enjoy all of the previously mentioned desirable characteristics, but they also exploit simple and universal interpolating basis functions, further enhancing their effectiveness. However, they require that the functions to represent must be *band-limited*. Therefore, we are led to the following question:

How and to what extent can radiated fields be effectively represented in terms of band-limited functions?

The approach adopted by Bucci and coworkers to answer this question and the main results are summarized and discussed in the next section.

EFFECTIVE FIELD BANDWIDTH AND SAMPLING REPRESENTATION

Let us first consider the case of a 1D observation domain, namely a closed analytic curve. The basic idea for developing an effective sampling representation [6] was to adopt

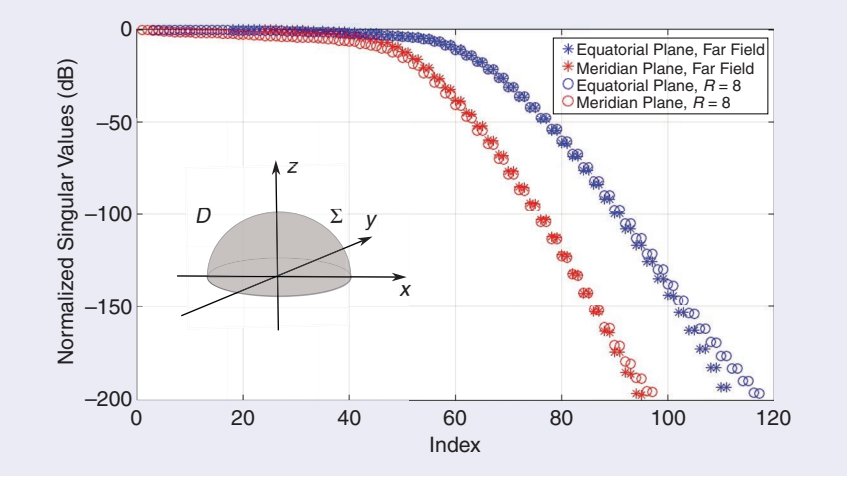

FIGURE 3. Singular values of the radiation operator of a semispherical source of radius 5 λ on meridian and equatorial circumferences having radius 8 λ and in far field. Inset: The geometry of the source.

a proper parameterization of the curve, say $\mathbf{r} = \mathbf{r}(\xi)$, and a proper phase factor $\exp[i\psi(\xi)]$ in such a way that the *reduced field*

$$F(\xi) = \exp[j\psi(\xi)]E(\mathbf{r}(\xi)) = \int_D \exp[j\psi(\xi)]G(\xi, \mathbf{r}')J(\mathbf{r}')d\mathbf{r}' = \int_D \hat{G}(\xi, \mathbf{r}')J(\mathbf{r}')d\mathbf{r}' \quad (6)$$

can be approximated best with a band-limited function.

As $F(\xi)$ is periodic, without loss of generality we can assume that the period is equal to 2π. Hence, the best band-limited approximations, say F_N, are obtained by truncating its Fourier series to the $2N+1$ harmonics of order $\leq N$, which amounts to (circularly) convolving F with the Dirichlet kernel:

$$D_N = \frac{1}{2\pi} \frac{\sin\left[\frac{(2N+1)\xi}{2}\right]}{\sin\left(\frac{\xi}{2}\right)}. \quad (7)$$

Accordingly, taking (6) into account, we have

$$F_N(\xi) = D_N(\xi) * F(\xi) = \int_D D_N(\xi) * \hat{G}(\xi, \mathbf{r}')J(\mathbf{r}')d\mathbf{r}' = \int_D \hat{G}_N(\xi, \mathbf{r}')J(\mathbf{r}')d\mathbf{r}' \quad (8)$$

where $*$ denotes convolution and $\hat{G}_N(\xi, \mathbf{r}')$ the band-limited version of the reduced Green function.

Paralleling [4], $\Delta\hat{G}_N = (\hat{G}_N - \hat{G})$ can be asymptotically evaluated as a function of N and ξ in the high-frequency limit, by splitting $\sin[(2N+1)\xi/2]$ in (7) into exponentials and applying, in the complex ξ-plane, the steepest descent method to the corresponding integrals. The saddle points are given by the condition

$$\pm\left(N+\frac{1}{2}\right) + \frac{\partial}{\partial\xi}[\psi(\xi) - \beta|\mathbf{r}(\xi) - \mathbf{r}'|] = \pm\left(N+\frac{1}{2}\right) + \frac{\partial}{\partial\xi}\gamma(\xi, \mathbf{r}') = 0 \quad (9)$$

β being the propagation constant.

For $(N+1/2) < \max_\xi|(\partial/\partial\xi)\gamma(\xi, \mathbf{r}')|$, there are at least a couple of real saddle (i.e., stationary phase) points. If ξ is between them, when the integration path is deformed into the steepest descent one, a pole (due to the $\sin(\xi/2)$ term in $D_N(\xi)$) is crossed, implying the presence of a residue equal, apart for a phase factor, to $\hat{G}(\xi, \mathbf{r}')$, and hence a large error. In the opposite case, the saddle points are complex, and the corresponding contributions go asymptotically to zero faster than any power as N increases, as long as the adopted parameterization and phase function do not introduce spurious singularities on the real axis.

Therefore, if we want to ensure a small error whatever the source current distribution, we must enforce the condition

$$N > \max_{\mathbf{r}'}\left(\max_\xi\left|\frac{\partial}{\partial\xi}\gamma(\xi, \mathbf{r}')\right|\right) - \frac{1}{2} = \max_\xi\left(\max_{\mathbf{r}'}\left|\frac{\partial}{\partial\xi}\gamma(\xi, \mathbf{r}')\right|\right) - \frac{1}{2} = W. \quad (10)$$

Hence, the band-limitation error exhibits a step-like behavior: large for $N < W$ and rapidly decreasing as N exceeds W. Accordingly, if we want to minimize the number of harmonics required to approximate the field, we must choose $\psi(\xi)$ and $\xi(\mathbf{r})$ in such a way as to minimize the critical bandwidth W.

As shown in [6], this leads to the following expressions for ψ and ξ:

$$\psi(\xi) = \frac{\beta}{2}\int_0^s\left[\max_{\mathbf{r}'}\left(\frac{\partial R}{\partial s}\right) + \min_{\mathbf{r}'}\left(\frac{\partial R}{\partial s}\right)\right]ds + \text{const} \quad (11)$$

$$\xi(\mathbf{r}(s)) = \frac{\beta}{2W_0}\int_0^s\left[\max_{\mathbf{r}'}\left(\frac{\partial R}{\partial s}\right) - \min_{\mathbf{r}'}\left(\frac{\partial R}{\partial s}\right)\right]ds + \text{const} \quad (12)$$

where s denotes the arc length, $R = |\mathbf{r}(s) - \mathbf{r}'|$, and W_0 is the corresponding minimal critical bandwidth, determined by enforcing that, for s equal to the curve length, ξ equals 2π. It turns out, as detailed in the following, that W_0 is proportional to the source size in wavelengths.

Exploiting, as in [4], the corresponding asymptotic expression of $\Delta\hat{G}_N$, it can be shown that, after the knee, the relative band-limitation error decreases as

$$\exp\left[-cW_0\left(\frac{N}{W_0} - 1\right)^{\frac{3}{2}}\right] = \exp\left[-\left(\alpha\frac{2N - 2W_0}{\sqrt[3]{2W_0}}\right)^{\frac{3}{2}}\right] \quad (13)$$

the constant α depending only on the source and curve geometry. This implies that, for large sources, a small relative increase of the bandwidth with respect to W_0, depending only logarithmically on the required precision, ensures a practically negligible band-limitation error. Accordingly, W_0 can be naturally identified with the (reduced) field effective bandwidth.

Now, while F_N can be *exactly* represented via a sampling expansion involving $2N+1$ samples, we are looking for a sampling representation of F, which is not exactly band-limited. Exploiting its samples, instead of those of F_N, introduces an aliasing error. However, it can be shown [5] that this aliasing error is at most about 40% larger than the band-limitation one, so that it can be counteracted by marginally increasing N.

Therefore, we conclude that by adopting an oversampling ratio $\chi = N/W_0$ slightly larger than one, $F(\xi)$, hence $E(\xi)$, can be accurately represented with a sampling expansion involving $2N+1$ samples, uniformly spaced in ξ.

We must find the functions ψ and ξ exploiting relations (11) and (12) to apply the preceding results. This can be done in the case of rotationally symmetric sources, with reference to arbitrary curves lying in meridian planes [6], reducing the evaluation of ψ and ξ to that of quantities having a simple geometrical meaning. It turns out that the values of ψ and ξ at a point depend only on the point itself and not on the curve through it. Hence, in any meridian plane, the couple (ψ, ξ) provides a "natural" coordinate system, which is orthogonal.

Moreover, the variation of ξ along a curve encircling the source is always equal to $\beta l/W_0$, l being the length of the intersection of the meridian plane with Ξ. Accordingly, for any meridian curve, the effective bandwidth, $W_{0\xi}$, is equal

to $\beta l/2\pi = l/\lambda$, so that the number of samples required to represent F is practically constant, even in the limit of an *unbounded curve*.

Due to the rotational symmetry, the azimuthal angle ϕ provides the optimal parameterization for azimuthal circles. They are the obvious coordinate curves to adopt to complete the "natural" coordinate system. The corresponding effective bandwidth, $W_{0\phi}$, depends only on ξ and is equal [6] to $\beta\rho_\xi$, ρ_ξ being the radial coordinate of the intersection of the corresponding ξ coordinate line with Ξ.

Exploiting the preceding results, we can obtain a sampling representation of the field on *any* surface Σ with the same rotational symmetry of the source, involving samples lying on $[\chi W_{0\xi}] = [\chi l/\lambda]$ azimuthal circles uniformly spaced in ξ, each one with $[\chi 2\beta_{\rho\xi}]$ uniformly spaced samples, $[\cdot]$ denoting the integer part. For large sources, the overall number of samples turns out to be nearly equal to $\chi^2 \mathcal{N}_0$, where $\mathcal{N}_0 = \text{area}(\Sigma)/(\lambda/2)^2$ [6].

Notwithstanding its relevance, this result is not enough because the computation of a field value with a standard cardinal series (with Dirichlet sampling functions), which involves all of the samples, is computationally demanding. We can overcome this difficulty by exploiting a central interpolation scheme exploiting *self-truncating* sampling functions [19], [20], requiring an increase of the sampling rate and retaining only the samples in a fixed neighborhood of the output point. This leads to what is called *optimal sampling interpolation* (*OSI*) [21]. Using only near samples introduces a truncation error, which can be effectively controlled by a proper choice of the sampling rate increase and of the number of retained near samples. Notably, the availability of an explicit sharp upper bound for the truncation error [21] allows optimizing such a choice.

Anyway, the increase in the overall number of required field samples is largely compensated by the strong reduction of the computational burden for field evaluation. Moreover, the fact that only nearby samples are required to evaluate the field implies that, if we are interested in evaluating the field only in a part of Σ, we have to compute or measure only a fraction of the overall samples. Last, but not least, the local nature of the interpolation avoids the propagation of unavoidable errors on the samples from high to low field values, as happens when using the standard cardinal expansion.

Coming back to vectorial fields, the preceding results are clearly valid for each field component, so the OSI representation can be directly applied to them, in particular to the tangential ones, to be exploited for evaluating the external field.

Leaving aside the increase in the sampling rate required to control the truncation error in the OSI, the last point to address is the redundancy of the cardinal sampling representation with respect to the optimal one, i.e., how much larger with respect to NDF_ϵ is the number of samples required to achieve the same precision?

In the case of azimuthal circles, the answer is obvious as the rotational invariance implies that the optimal parameterization is given by ϕ, and the right singular functions are the normalized exponentials $(1/\sqrt{2\pi})\exp(\pm jn\phi)$, so that (apart, possibly, for the order) singular values and band-limitation errors coincide.

In the case of arbitrary meridian curves, as singular values and band-limitation errors share the same step-like behavior, it is reasonable to think that the difference after the knee will mainly depend on the ratio between $2W_0$ and the critical index, say n_0, of the singular values and on the ratio of the decrease rates after the knee. To check this point, it is convenient to report the singular values, normalized to the singular value at $[2W_0]$, as a function of the normalized index $\nu = n - 2W_0/\sqrt[3]{2W_0}$ appearing in the asymptotic expression (13) of the band-limitation error. As a typical example, we report in Figure 4 the graphs relative to the case of the hemisphere far field considered in Figure 3. Apart from the first one, all of the singular values are doubly degenerate, so we report only the singular values of odd index.

As can be seen, the normalized singular values relative to the equatorial and meridian cuts are practically parallel near $\nu = 0$, with a slight shift of about 1 dB. Moreover, the behavior of the singular values after the knee is quite similar, the difference appearing proportional to ν, as happens for the band-limitation error; see (13). Indeed, a shift of 1 dB and a simple 7% increase of the abscissa scale will bring the meridian values to fit the equatorial ones, as shown in the same Figure 4.

Such results, in particular the fact that n_0 is nearly equal to $2W_0$, show that, leaving aside the oversampling required to control the aliasing error, there are two main factors affecting the redundancy of the cardinal sampling representation. The first is the value of the constant α appearing in (13), which, for meridian curves, is expected to be smaller in the case of the band-limitation error. The second, more subtle, factor is the occurrence of singularities on or near the real axis of the complex ξ-plane if the intersection of the meridian plane with the surface Ξ of the source is not analytic or has sections with strong curvature. This occurrence can deeply affect the asymptotic behavior of the band-limitation error, possibly destroying its exponential decay.

To clarify these points, let us consider a circular array of radius 5 λ, consisting of $\lambda/4$-spaced, z-directed elementary dipoles,

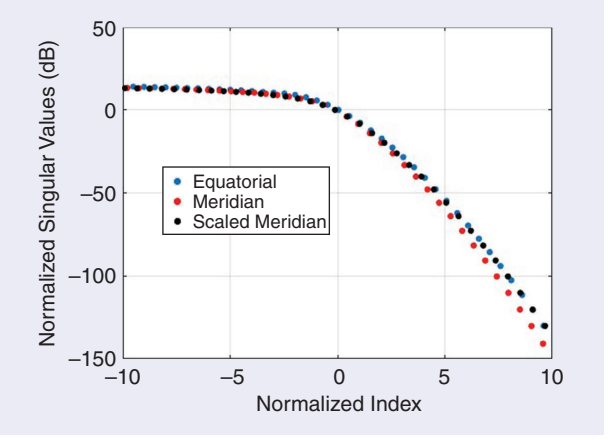

FIGURE 4. Singular values, normalized to the singular value at $2W_0$, of the far-field radiation operator of the semispherical source as a function of the normalized index ν.

as depicted in the inset of Figure 5, and the corresponding far fields in the coplanar $(y-z)$- and equatorial $(x-y)$-planes. In the first case, no singularity is present in the finite complex ξ-plane, while in the second, two singularities are present on the real axis for $\xi = \pm\pi/2$, so that the two cases represent the extreme possibilities.

Figure 5 reports, as a function of the bandwidth N, the Green function normalized band-limitation error, $\|\Delta\hat{G}_N\|/\|\hat{G}\|$, and that corresponding to SVD truncation to $2N+1$ terms. As can be seen, in the coplanar case, after the knee ($W_0 = 31$), the band-limitation and the SVD truncation errors run parallel, confirming the expected equal exponential decay, while in the equatorial case ($W_0 = 20$), they detach, the band-limitation one exhibiting a much slower power law decay.

The most natural and straightforward way to counteract such degradation is to include the array in a domain D of the same size and symmetry of the array but bounded by an analytic surface Ξ, to move the singularities outside the real axis of the corresponding complex ξ-plane. A convenient and flexible choice

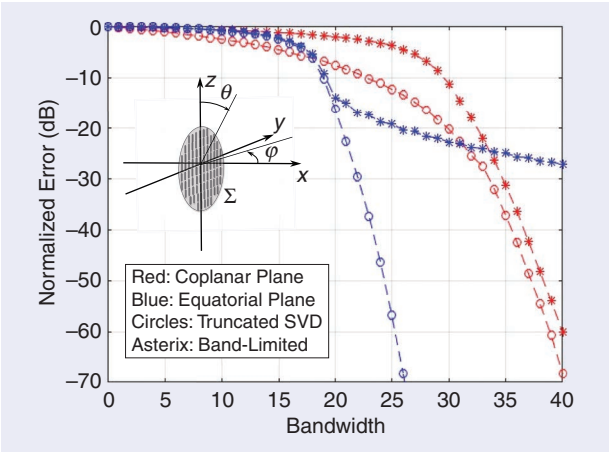

FIGURE 5. Band-limitation and SVD truncation errors for the array far-field Green function. Inset: The geometry of the problem.

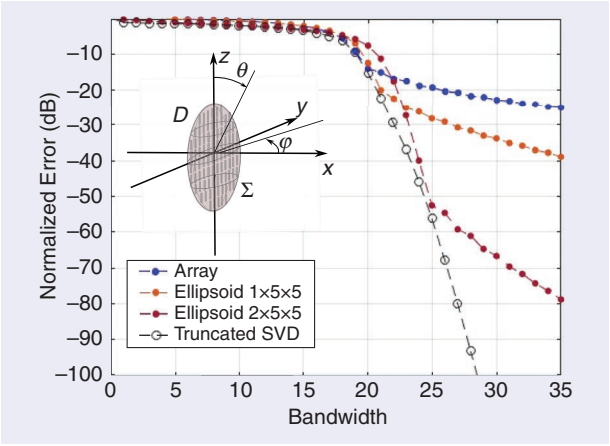

FIGURE 6. Band-limitation error of the array equatorial Green function for two values of the minor semiaxis of the ellipsoidal domain D. For comparison, the SVD truncation error is also plotted. Inset: The geometry of the problem.

is that of an oblate spheroid, for which an explicit expression of $\xi(\mathbf{r})$ is available [6]. Figure 6 reports the normalized band-limitation error of the equatorial Green function for two values of the minor semiaxis, namely 1λ and 2λ. For comparison, we also report the SVD truncation error. The effect of increasing the spheroid thickness is evident. There is a slight increase of the value of W_0, which is largely compensated by the decrease in the error value at the detachment of the band-limitation error from the exponential decay. In particular, in the case of a half thickness of 2λ, this happens for $W = 25$, with a band-limitation error of –53 dB, 34 dB lower than the corresponding error of Figure 5 and just 3 dB larger than the SVD truncation one.

Moreover, we must take into account that the Green function normalized band-limitation error is the least upper bound for the error we made when considering an arbitrary source in the unit ball X, while only a subset of all possible current distributions in X can be actually realized, namely that of *nonsuperdirective* sources.

As is well known, a (linear or planar) source is called *superdirective* if its directivity significantly exceeds that of a uniformly excited one. This implies a large *superdirectivity ratio* (*SDR*), namely the ratio between the total (real plus reactive) and real radiated power,[3] which requires a strong increase of both the intensity of the source and the accuracy in its realization [24]. Accordingly, superdirectivity is limited by physical (maximum source power, efficiency, etc.) and realization constraints (manufacturing tolerances, feeding network accuracy, etc.) as well as by the required bandwidth. Hence, the band-limitation error of an actual source could be significantly lower than the least upper bound.

To analyze this point, let us consider again two extreme cases, namely a uniform-amplitude, random-phase excitation and a uniform-amplitude, constant-phase one. In the first case, because of the small elements separation, there is an aggressive exploitation of the DOF with a quite large SDR, while in the second case, the SDR is slightly larger than one.

Figure 7 reports the corresponding band-limitation errors for a spheroid half-thickness equal to 2λ as well as, for comparison, the SVD truncation error of the Green function. For $W = 25$ in the random array case, the error is –58 dB, 5 dB lower than the Green function band-limitation error and also slightly lower than the SVD truncation one, while in the case of the uniform array, the error is –85 dB, a full 29 dB lower than the SVD truncation one. The far-field pattern of the random array is reported in Figure 8, together with the band-limitation error patterns for $W = 25$ when adopting the preceding spheroidal domain or a flat one. The dramatic reduction of the error, particularly in the neighborhood of the critical points $\pm\pi/2$, is evident.

The theory reported in this section has been validated by the large amount of numerical and experimental studies reported in the following section, particularly in the areas of antenna measurement and synthesis.

In conclusion, for all cases of practical interest, involving sources with reasonable superdirectivity and realistic required

[3]The concept and the original Taylor's definition [22] of superdirectivity can be easily extended to arbitrary sources and observation domains [23].

precision, the redundancy of the OSI representations along the meridians and parallels of an observation surface with the same rotational symmetry of the source is essentially due to the oversampling factors required to control the aliasing and truncation errors. Hence, the band-limitation theory provides a reliable estimate of n_0, i.e., the effective rank of the corresponding radiation operators. However, this does not imply that the same happens when building a 2D OSI representation exploiting the coordinate curves of the natural system (ξ, ϕ) over the observation surface. In the case of the far field of spherical or circular planar sources, explicit expressions for the SVD critical index n_0 in the high-frequency limit can be obtained, exploiting, respectively, the spherical wave expansion of the field and the Landau theorem [25]. It turns out that the ratio between the number of samples at the Nyquist rate and n_0 is equal to $4/\pi$, entailing a corresponding increase of the OSI redundancy.

Of course, for large sources, this redundancy increase does not impair the effectiveness of the OSI representation, but it should be taken into account when estimating the NDF or the radiation operator effective rank.

It must be stressed that, because of its local nature, OSI can also be adopted to represent the field on a *part* of the observation curve or surface, exploiting just a few extra samples outside the domain of interest. Accordingly, the preceding considerations and results also stay valid in this case, so that it is possible to estimate the NDF and the effective rank of the radiation operator in this case too, by just counting the samples falling inside this domain. This allows us to investigate, in a simple way, the dependence of the effective rank of the radiation operator describing the interaction of a source with a confined observation region on both the sizes of the source and the domain as well as their relative geometry.

As emphasized in the section "Introduction," the problem of efficiently representing the electromagnetic field is strictly related to the identification of the "amount of information" associated to the set of the electromagnetic field configurations radiated by the source. Consequently, it is not surprising that the theory has important connections with information theory [26]. Indeed, the field approximation is straightforwardly related to the distortion theory [27], which addresses the problem of determining the minimum number of bits required to transmit or store information subject to a certain level of distortion. Furthermore, even if the analysis carried out up to this point is focused on the problem of representing the electromagnetic field, it can also be extended with minimal effort to the problem of identifying the maximum amount of information that can be transmitted by electromagnetic fields. In fact, the two problems are closely linked.

Considering the problem of information transmission, the objective is to find the least upper bound of the number of field configurations that can be distinguishable on Σ in the presence of uncertainty ϵ. The solution requires the packing of Y by means of open balls. The least upper bound of the number of balls is the Kolmogorov capacity or metric capacity [28].

The Kolmogorov functional approach has a number of relevant applications in modern MIMO communication systems. These systems employ space–time modulation, where independent streams of bits are transmitted along spatially uncorrelated subchannels [29]. With reference to the functional representation outlined in the section "DOF of the Electromagnetic Field," each stream of bits is transmitted using the basis $\{e_1, \ldots, e_k, \ldots\}$. Consequently, the number of spatial subchannels that can be utilized in spatiotemporal coding is limited by NDF_ϵ [9]. Optimal sampling theory not only provides a simple estimate of the maximum number of subchannels in MIMO communication systems but also offers a graphical representation of how to place the elements of the receiving antenna to efficiently utilize the number of potentially available spatial subchannels, which are given by the sampling points of the spatial area available to the receiving system [9].

More generally, the theory provides constraints on the amount of transmission of communication systems related to the analytical properties of the fields. The study of these constraints and the practical consequences in communications systems is the object of research of the EIT.

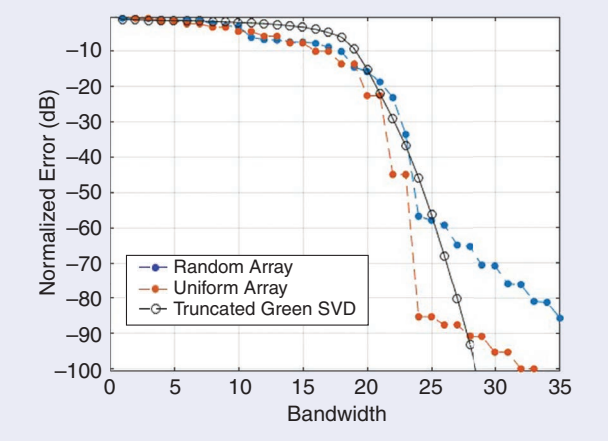

FIGURE 7. Array equatorial band-limitation errors for random phase and uniform excitation, with 2λ spheroid thickness. For comparison, the SVD truncation error of the Green function is also plotted.

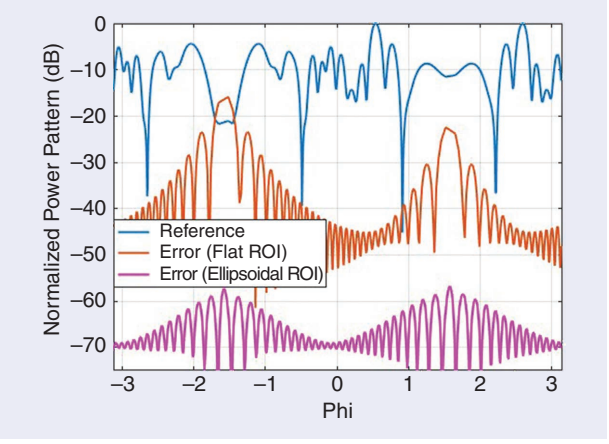

FIGURE 8. Equatorial pattern of the random array and band-limitation error patterns for $W = 25$ in the case of a flat and an ellipsoidal domain D.

APPLICATIONS

To review and briefly discuss the main applications of the theory and results reported in the preceding sections, it is convenient to consider separately "direct" and "inverse" electromagnetic problems.

In the case of direct problems, namely the evaluation or measurement of the field radiated by a given source or scattered by a given scatterer, the availability of effective and nonredundant sampling representations allows us to minimize the computational and/or the measurement burden. Therefore, the most obvious application of the sampling theory, which motivated its original development [30], [31], is the numerical evaluation of the fields radiated or scattered by electrically large structures [21], [32], [33], particularly in the context of fast integral equation solvers [34], [35], [36], [37], [38], [39], [40]. Moreover DOF theory allows for the identification of blocks of moment matrices to be compressed and for the efficient processing of their low rank approximations [41]. Furthermore, the availability of a reliable estimate of the field NDF allows us to assess the minimal computational complexity of radiation or scattering problems, providing a benchmark for any specific algorithm [42].

For antenna synthesis, it is clear that the overall dimension of the space of the excitation and design parameters should match the NDF of the field of the source (given its size and shape).

As highlighted at the end of the section "DOF of the Electromagnetic Field," sampling representations exploiting OSI are particularly attractive in the case of radiated field measurements, in particular, antenna near-field measurements.

In near-field measurements, the field radiated by the antenna under test (AUT) is probed on a proper scanning surface placed in the near-field area and processed to obtain information on the field configuration in far field. The procedure is extremely effective, but it is not free from important challenges, such as the time required to acquire the data in cases of electrically large antennas, the presence of environmental reflections, and the constrained measurement zone present in some scanning configurations, such as the planar and cylindrical ones [43].

Nonredundant sampling is a powerful tool for reducing these problems. In fact, the theory provides the optimal number of samples and their positions required for a fast and accurate reconstruction of the field on essentially arbitrary scanning surfaces. In such a way, the measurement time can be significantly reduced, while allowing a "transparent" adoption of the standard near-field-to-far-field transformation algorithms. Moreover, it is possible to adopt scanning geometries and/or procedures different from the canonical planar, cylindrical, and spherical ones, allowing a further reduction of the measurement time. Particularly interesting unconventional scanning procedures include large-mesh planar scanning [44], bipolar scanning [45], [46], helicoidal scanning [47], planar spiral [48], and plane-polar techniques [49]. The theory also allows identifying the optimal location of probes in multiprobe antenna measurement systems, an architectural solution particularly suited for very fast measurements of 5G and 5GB millimeter-wave antenna patterns [50]. An up-to-date and comprehensive description of the applications to near-field measurements in both canonical and nonconventional scanning geometries is provided in [51].

Notably, under fairly reasonable conditions, it is also possible to exploit nonuniformly spaced field samples [32], [52]. Moreover, using mathematical techniques developed in the framework of linear inverse problems, sampling theory can also be exploited to estimate the field outside the physical extension of the scanning area, reducing the truncation errors in the far-field evaluation [53]. The method has been successfully applied to base station antenna measurement using cylindrical near-field scanning surfaces [54]. In this approach, the minimum redundancy of the representation plays a crucial role, reducing the number of samples to be estimated, or also completely avoiding the truncation by identifying the positions among the ones accessible by the scanning system that carry the missed information [55].

Sampling representation has also been used in near-field-to-far-field transformation from only amplitude data, an important topic in millimeter-wave and sub-terahertz antennas proposed for the next generation of personal communication systems [56]. The theory has also been successfully applied to near-field measurements in the time domain [57], [58] and to radar cross-section problems [59] as well as to compressed sensing, achieving a further reduction in the number of samples required for the representation of the field in the case of sparse sources [60].

Lastly, the nonredundant sampling theory allows us to improve the performance of the measurement set through signal processing techniques, by exploiting the extensive literature developed for numerical signal processing. As an example, all of the noise that falls outside the spatial bandwidth of the AUT can be filtered out by oversampling the field and filtering the spatial harmonics falling outside the spatial bandwidth of the AUT. The procedure gives quite effective results. In fact, the ξ-parameterization is optimized to reduce the bandwidth of the sources inside the volume of the AUT, while it tends to enlarge the spatial bandwidth of sources placed *outside* this volume. Consequently, the energy of spatial harmonics of the interference sources tends to be outside the spatial bandwidth of the AUT, making the filtering process more effective [61].

Regarding inverse problems, such as antenna synthesis and inverse scattering, the main difficulty we must face is their intrinsic ill-posedness (or, at least, ill-conditioning), which implies high sensitivity to noise, measurement errors, and realization tolerances. Therefore, the knowledge of the NDF of the involved fields and the exploitation of nonredundant field

representations is of paramount importance to get feasible and/or reliable results, without unnecessarily limiting the space of the possible solutions.

To this end, for antenna synthesis, it is clear that the overall dimension of the space of the excitation and design parameters should match the NDF of the field of the source (given its size and shape), as happens in the case of classical $\lambda/2$-spaced linear or planar arrays.

Particularly relevant is the fact that the band-limitation theory allows us to formulate a simple and effective necessary condition for assessing the *existence* of a nonsuperdirective source, of given size and shape, capable of radiating a power pattern lying in an arbitrary mask, without actually solving the synthesis problem [62]. Indeed, the fact that the squared amplitude of a band-limited function is also band-limited, with doubled bandwidth, implies that the feasible patterns satisfying the constraints must belong to the intersection of two convex sets, namely the set of the real band-limited functions (of doubled bandwidth) and that of the nonnegative real functions lying in the mask. The existence of a nonvoid intersection can be ascertained by solving a convex problem, for which flexible and effective algorithms (as the alternate projections algorithm [63], [64]) are available. In the positive case, we get a possibly feasible power pattern, which can be profitably exploited for the source synthesis. In the opposite case, we must relax the constraints or increase the source size until they can be met, thus allowing us to fit the antenna size to the power pattern requirements.

Notably, the feasibility criterion is also sufficient in the 1D case of linear or circularly symmetric sources. The power pattern synthesis problem can be completely solved by exploiting convex optimization techniques to determine the optimal power pattern, followed by a polynomial factorization to find the corresponding (possibly not unique) source [62], [65]. The source so obtained can be profitably exploited to synthesize a sparse, *equiamplitude* array, of particular interest for satellite TLC [66], using fast deterministic procedures [67], [68], and for the synthesis of plane-wave generators [69].

The field DOF and the source SDR play an even more major role in the case of antennas whose goal is to deliver, in a controlled way, power and not information inside a given region of interest (ROI), as, for instance, in clinical hyperthermia [70]. The design of such an antenna, typically an array, must face fundamentally different issues and constraints in comparison to those of the "classic" design of arrays for telecommunications [23].

First, the ROI is a 3D domain, located in the near-field zone of the array, which is possibly embedded in a matching medium. The fact that the ROI is 3D implies that the closure of the range of the radiation operator is a proper subspace (of infinite codimension) of L^2 (ROI), thus strongly limiting the set of radiable fields. In particular, even accepting arbitrarily large SDRs, we cannot improve at will the field shaping or focusing, as happens in the case of TLC applications, usually dealing with far fields, and hence 2D ROI.

Second, the geometry of the array depends on the anatomy of the considered part of the body and must be conformal to it to improve coupling and penetration.

Finally, the ROI is electrically heterogeneous and lossy, and its features *vary from patient to patient*. Hence, to allow patient and treatment specificity, the exposure system must be *reconfigurable* to deal with changes in both the electrical properties of the ROI and the required power density distribution. Since, in practice, such a reconfigurability can be obtained only by exploiting the array excitations, the array layout, namely the number and location of its elements, must be necessarily designed *in advance*, relying on the knowledge of the overall geometry of the ROI and of the array as well as of the electromagnetic parameters of the matching medium. Accordingly, given the operating frequency, the element type, and the *maximum allowable SDR*, the design goal is to maximize, exploiting such knowledge, the array reconfigurability, i.e., the dimension of the space of the fields radiated in the ROI. However, because, as stressed before, the 3D reconfigurability is limited, irrespective of the source SDR, the layout design must aim at minimizing the number of array elements while ensuring a satisfactory focusing effectiveness.

A possible design procedure is presented in [23] and applied to the design of a system for the hyperthermia treatment of breast cancer.

Once the array layout has been designed, the excitations required to best focus the field within the ROI can be determined by solving a relatively "standard" (even if numerically cumbersome) synthesis problem, for which numerous techniques are available [23] (see, f.i. references 20–27 of [23]).

Regarding inverse scattering problems, wherein the goal is to recover the electromagnetic contrast[4] of a scatterer from scattering measurements performed with illuminating and measuring probes lying on a surface surrounding the ROI, a fundamental question to address concerns the maximum amount of information that can be reliably retrieved from scattering measurements and how it can be effectively collected.

As shown in [71], band-limitation theory and the corresponding sampling representations allow us to give the following general answer to this question.

The maximum amount of information that can be reliably collected in the most general scattering experiment (double polarization, multisource, multiview) cannot significantly exceed $M_0 = 2(N_0^2/2)$, N_0 being the number of $\lambda/2$ spaced points on the boundary of the smallest rotationally symmetric domain containing the ROI. The information can be effectively collected by positioning the illuminating and measuring probes in the Nyquist lattice in the canonical variables (ξ, ϕ) corresponding to the surface Ξ.

Exploiting such information, the scattering matrix elements can be evaluated (within the measurement precision) for arbitrary positions of the illuminating and measuring probes via a double sampling expansion, thus ensuring that all of the collectable information is captured. However, this provides only an upper bound to the amount of information on the scatterer contrast that we can retrieve. Because the inverse scattering

[4]As is well known, in the usual case of nonmagnetic scatterers, the contrast is just the relative difference between the scatterer equivalent permittivity and that of the background.

problem is ill-conditioned and the scattering operator, namely the operator relating the contrast to the scattering matrix, is nonlinear, so that the SVD machinery is unavailable, it is challenging to determine how much of the information on the contrast encoded in the scattering matrix can be recovered and how this can be done.

An exception is the case of contrast near to zero (weak scatterers), for which we can linearize the operator by approximating the field inside the scatterer with the incident field (Born approximation), thus allowing us to determine the essential dimension, say P, of the space of the scattering matrices and hence the actual amount of information on the contrast they encode.

In the particular case of far-field scattering, it turns out [71] that while in the 2D case the ratio M_0/P is larger than one (as expected), but independent of the ROI size, in the 3D case this ratio increases linearly with the size. This happens because, under the Born approximation, the scattering matrix is a function of the sum of the incident and scattering directions and not of those directions separately, which induces a strong linear dependence between the elements of the scattering matrix and a consequent lowering of the retrievable information.

Assessing the amount of this reduction and its possible persistence when the weak scattering hypothesis is removed is a hard problem. By linearizing the scattering operator around a given contrast (distorted Born approximation) or exploiting a second-order Born approximation [72], [73], one can numerically investigate the problem in specific, possibly simplified, scenarios, gaining insights on the influence of the contrast characteristics on the achievable resolution. However, to the best of our knowledge, notwithstanding its great theoretical and practical interest, a general and satisfactory analysis is still lacking.

Finally, as noted in the section "Introduction," the theory described is a powerful tool for understanding the relationships between information and electromagnetic fields [9], [11], [74], [75], [76], [77], [78], [79]. The associated research area (EIT) serves as a foundational basis for exploring innovative strategies in wireless communications. A notable development is the emergence of a new research field known as *electromagnetic signal processing and information theory* (*ESIT*) [80]. ESIT includes the manipulation of the electromagnetic field within the communication channel through the utilization of intelligent passive or active scattering devices. The band-limitation theory of electromagnetic fields allows us to immediately use the vast literature developed for signals in the time domain to the spatial configuration of the electromagnetic field. Applications of ESIT include the fast-growing field of reflecting intelligent surfaces [81], intrinsically secure communications [82], and in general the control of the communication channel [7].

The availability of a simple and universal "bridge" has allowed researchers to focus resources toward applications, leading to the plethora of solutions briefly listed in this work.

The connections between electromagnetism and information could appear to be only an exciting and intriguing academic field of research. However, on the contrary, this topic has important implications in modern society. As an example, the modern information society is characterized by immense amounts of data transmitted via electromagnetic phenomena. But the other side of the coin is the enormous energy consumption associated with data transmission. The theory of DOF and the approximation by band-limited functions of the fields represent a tool to identify solutions to transmit information with lower energy, opening new perspectives for more environmentally suitable wireless communication networks.

CONCLUSIONS

One characteristic that catches the eye when looking at the path that led to the development of the sampling representation of the electromagnetic field is certainly the rigorous and elegant mathematical structure underlying the theory, which was clearly defined from the very beginning. This theory has provided robust pillars for the development of analytical formulas that allow the estimation and control of the representation error. This is particularly valuable from an engineering point of view, making the theory a flexible and reliable tool. However, there is another noteworthy feature of the theory: the number of applications in which it is useful. Its pervasiveness in and outside the field of electromagnetism represents in itself a significant result, deserving of careful consideration.

Starting from the brief observations reported in the section "Introduction," the representation of the electromagnetic field represents a "bridge" that connects the mathematical description of electromagnetic phenomena provided by Maxwell's equations to the real world. Loosely speaking, any field representation takes advantage of some a priori information on the problem of interest to reduce the number of parameters required to represent the set of radiated or scattered fields. However, including complex a priori information has a cost in terms of the complexity of the representation. The band-limited representation requires a few pieces of easily available a priori information on the electromagnetic source, i.e., its dimension, shape, and position in space. Following the analogy of the bridge, this representation is the equivalent of a prefabricated bridge: an economical, simple, and universal solution, resting on the robust pillars of a rigorous mathematical framework. The advantage is the same as that of a prefabricated bridge in the realization of a complex communication infrastructure: it allows the concentration of available money and energy toward other parts of the infrastructure. Furthermore,

given the previously recalled a priori information, the representation is almost optimal in terms of the number of samples required to represent the field. In other words, we would not have significant improvements if, given the a priori conditions mentioned previously, we decided to design and build an ad hoc bridge—we would obtain only a waste of time and money.

Briefly, the availability of a simple and universal "bridge" has allowed researchers to focus resources toward applications, leading to the plethora of solutions briefly listed in this work. In conclusion, never underestimate the usefulness of a good bridge, especially if we want to leave the plain and reach the summit of the highest mountain.

AUTHOR INFORMATION

Ovidio Mario Bucci (bucci@unina.it) is a professor emeritus at the University of Naples Federico II, 80138 Naples, Italy. His scientific interests include theoretical electromagnetism, antenna analysis, synthesis and measurements, noninvasive diagnostics, and biological applications of electromagnetic fields. He is a Life Fellow of IEEE.

Marco Donald Migliore (mdmiglio@unicas.it) is a full professor in the Department of Electrical and Information Engineering, University of Cassino and Southern Lazio, 03043 Cassino, Italy, where he is director of the Microwave Laboratory. His research interests include electromagnetics, signal processing, and information theory, multiple-input, multiple-output antennas, sparse recovery applications, and applications of microwaves. He is a Senior Member of IEEE.

REFERENCES

[1] R. J. I. Marks, *Introduction to Shannon Sampling and Interpolation Theory*. New York, NY, USA: Springer-Verlag, 2012.

[2] G. Toraldo Di Francia, "Resolving power and information," *J. Opt. Soc. Am.*, vol. 45, no. 7, pp. 497–501, 1955, doi: 10.1364/JOSA.45.000497.

[3] H. J. Landau and H. O. Pollak, "Prolate spheroidal wave functions, fourier analysis and uncertainty—III: The dimension of the space of essentially time- and band-limited signals," *Bell Syst. Tech. J.*, vol. 41, no. 4, pp. 1295–1336, Jul. 1962, doi: 10.1002/j.1538-7305.1962.tb03279.x.

[4] O. Bucci and G. Franceschetti, "On the spatial bandwidth of scattered fields," *IEEE Trans. Antennas Propag.*, vol. 35, no. 12, pp. 1445–1455, Dec. 1987, doi: 10.1109/TAP.1987.1144024.

[5] O. M. Bucci and G. Franceschetti, "On the degrees of freedom of scattered fields," *IEEE Trans. Antennas Propag.*, vol. 37, no. 7, pp. 918–926, Jul. 1989, doi: 10.1109/8.29386.

[6] O. M. Bucci, C. Gennarelli, and C. Savarese, "Representation of electromagnetic fields over arbitrary surfaces by a finite and nonredundant number of samples," *IEEE Trans. Antennas Propag.*, vol. 46, no. 3, pp. 351–359, Mar. 1998, doi: 10.1109/8.662654.

[7] M. D. Migliore, "Classical and quantum processing in the deep physical layer," *IEEE Access*, vol. 11, pp. 52,969–52,982, 2023, doi: 10.1109/ACCESS.2023.3280452.

[8] A. N. Kolmogorov and V. M. Tikhomirov, "ε-entropy and ε-capacity of sets in functional spaces," *Uspekhi Matematicheskikh Nauk*, vol. 14, no. 2, pp. 3–86, 1959, (English Transl.: AMS Transl., Ser. 2, vol. 17, 277–364, 1961).

[9] M. D. Migliore, "On the role of the number of degrees of freedom of the field in MIMO channels," *IEEE Trans. Antennas Propag.*, vol. 54, no. 2, pp. 620–628, Feb. 2006, doi: 10.1109/TAP.2005.863108.

[10] M. D. Migliore, "The world beneath the physical layer: An introduction to the deep physical layer," *IEEE Access*, vol. 9, pp. 77,106–77,126, 2021, doi: 10.1109/ACCESS.2021.3082772.

[11] J. Zhu, Z. Wan, L. Dai, M. Debbah, and H. V. Poor, "Electromagnetic information theory: Fundamentals, modeling, applications, and open problems," *IEEE Wireless Commun.*, vol. 31, no. 3, pp. 156–162, Jun. 2024, doi: 10.1109/MWC.019.2200602.

[12] Z. Wan, J. Zhu, Z. Zhang, L. Dai, and C.-B. Chae, "Mutual information for electromagnetic information theory based on random fields," *IEEE Trans. Commun.*, vol. 71, no. 4, pp. 1982–1996, Apr. 2023, doi: 10.1109/TCOMM.2023.3247725.

[13] D. S. Jones, *Acoustic and Electromagnetic Waves*," New York, NY, USA: Oxford Univ. Press, 1986.

[14] A. N. Kolmogorov and S. V. Fomin, *Elements of the Theory of Functions and Functional Analysis*, vol. 1. Rochester, NY, USA: GREAYLOCK Press, 1957.

[15] A. Pinkus, *n-Widths in Approximation Theory. A Series of Modern Surveys in Mathematics*, vol. 7. Berlin, Germany: Springer-Verlag, 1985.

[16] M. D. Migliore, "On electromagnetics and information theory," *IEEE Trans. Antennas Propag.*, vol. 56, no. 10, pp. 3188–3200, Oct. 2008, doi: 10.1109/TAP.2008.929444.

[17] C.-W. Ha, "Eigenvalues of differentiable positive definite kernels," *SIAM J. Math. Anal.*, vol. 17, no. 2, pp. 415–419, 1986, doi: 10.1137/0517031.

[18] C.-H. Chang and C.-W. Ha, "On eigenvalues of differentiable positive definite kernels," *Integral Equ. Operator Theory*, vol. 33, no. 1, pp. 1–7, 1999, doi: 10.1007/BF01203078.

[19] J. Knab, "Interpolation of band-limited functions using the approximate prolate series (Corresp.)," *IEEE Trans. Inf. Theory*, vol. 25, no. 6, pp. 717–720, Nov. 1979, doi: 10.1109/TIT.1979.1056115.

[20] J. Knab, "The sampling window (Corresp.)," *IEEE Trans. Inf. Theory*, vol. 29, no. 1, pp. 157–159, Jan. 1983, doi: 10.1109/TIT.1983.1056603.

[21] O. M. Bucci, C. Gennarelli, and C. Savarese, "Optimal interpolation of radiated fields over a sphere," *IEEE Trans. Antennas Propag.*, vol. 39, no. 11, pp. 1633–1643, Nov. 1991, doi: 10.1109/8.102779.

[22] T. T. Taylor, "Design of line-source antennas for narrow beamwidth and low side lobes," *Trans. IRE Professional Group Antennas Propag.*, vol. 3, no. 1, pp. 16–28, Jan. 1955, doi: 10.1109/TPGAP.1955.5720407.

[23] O. M. Bucci, L. Crocco, R. Scapaticci, and G. Bellizzi, "On the design of phased arrays for medical applications," *Proc. IEEE*, vol. 104, no. 3, pp. 633–648, Mar. 2016, doi: 10.1109/JPROC.2015.2504266.

[24] R. E. Collin, *Antenna Theory*. New York, NY, USA: McGraw-Hill, 1969.

[25] H. Landau, "On Szegö's eingenvalue distribution theorem and non-hermitian kernels," *J. d'Analyse Mathématique*, vol. 28, no. 1, pp. 335–357, 1975, doi: 10.1007/BF02786820.

[26] T. M. Cover, P. Gacs, and R. M. Gray, "Kolmogorov's contributions to information theory and algorithmic complexity," *Ann. Probability*, vol. 17, no. 3, pp. 840–865, 1989, doi: 10.1214/aop/1176991250.

[27] C. E. Shannon, "A mathematical theory of communication," *Bell Syst. Tech. J.*, vol. 27, no. 3, pp. 379–423, 1948, doi: 10.1002/j.1538-7305.1948.tb01338.x.

[28] V. Tikhomirov, "ε-entropy and ε-capacity of sets in functional spaces," in *Selected Works of A. N. Kolmogorov*, A. N. Shiryayev, Ed., Dordrecht, the Netherlands: Springer-Verlag, 1993, pp. 86–170.

[29] A. Paulraj, A. P. Rohit, R. Nabar, and D. Gore, *Introduction to Space-Time Wireless Communications*. Cambridge, U.K.: Cambridge Univ. Press, 2003.

[30] O. Bucci, G. Franceschetti, and G. D'Elia, "Fast analysis of large antennas–A new computational philosophy," *IEEE Trans. Antennas Propag.*, vol. 28, no. 3, pp. 306–310, May 1980, doi: 10.1109/TAP.1980.1142345.

[31] O. Bucci and G. Massa, "Exact sampling approach for reflector antennas analysis," *IEEE Trans. Antennas Propag.*, vol. 32, no. 11, pp. 1259–1262, Nov. 1984, doi: 10.1109/TAP.1984.1143230.

[32] O. M. Bucci, C. Gennarelli, and C. Savarese, "Interpolation of electromagnetic radiated fields over a plane by nonuniform samples," *IEEE Trans. Antennas Propag.*, vol. 41, no. 11, pp. 1501–1508, Nov. 1993, doi: 10.1109/8.267349.

[33] O. Bucci, C. Gennarelli, G. Riccio, and C. Savarese, "Sampling representation of electromagnetic fields over three-dimensional domains," *Radio Sci.*, vol. 34, no. 3, pp. 567–574, 1999, doi: 10.1029/1999RS900013.

[34] E. Michielssen and A. Boag, "A multilevel matrix decomposition algorithm for analyzing scattering from large structures," *IEEE Trans. Antennas Propag.*, vol. 44, no. 8, pp. 1086–1093, Aug. 1996, doi: 10.1109/8.511816.

[35] E. Michielssen, A. Boag, and W. C. Chew, "Scattering from elongated objects: Direct solution in o (n log2n) operations," *IEE Proc. Microw., Antennas Propag.*, vol. 143, no. 4, pp. 277–283, 1996, doi: 10.1049/ip-map:19960400.

[36] J. M. Rius, J. Parron, A. Heldring, J. M. Tamayo, and E. Ubeda, "Fast iterative solution of integral equations with method of moments and matrix decomposition algorithm–singular value decomposition," *IEEE Trans. Antennas Propag.*, vol. 56, no. 8, pp. 2314–2324, Aug. 2008, doi: 10.1109/TAP.2008.926762.

[37] A. Shlivinski and A. Boag, "Multilevel surface decomposition algorithm for rapid evaluation of transient near-field to far-field transforms," *IEEE Trans. Antennas Propag.*, vol. 57, no. 1, pp. 188–195, Jan. 2009, doi: 10.1109/TAP.2008.2009730.

[38] Y. Brick and A. Boag, "Fast direct solution of 3-D scattering problems via nonuniform grid-based matrix compression," *IEEE Trans. Ultrason.*,

Ferroelectr., Freq. Control, vol. 58, no. 11, pp. 2405–2417, Nov. 2011, doi: 10.1109/TUFFC.2011.2098.

[39] Y. Brick, V. Lomakin, and A. Boag, "Fast direct solver for essentially convex scatterers using multilevel non-uniform grids," *IEEE Trans. Antennas Propag.*, vol. 62, no. 8, pp. 4314–4324, Aug. 2014, doi: 10.1109/TAP.2014.2327651.

[40] Q. Gueuning, E. de Lera Acedo, A. K. Brown, and C. Craeye, "An inhomogeneous plane-wave based single-level fast direct solver for the scattering analysis of extremely large antenna arrays," *IEEE Trans. Antennas Propag.*, vol. 70, no. 10, pp. 9511–9523, Oct. 2022, doi: 10.1109/TAP.2022.3177465.

[41] Y. Brick and A. E. Y. Ilmaz, "Fast multilevel computation of low-rank representation of *H*-matrix blocks," *IEEE Trans. Antennas Propag.*, vol. 64, no. 12, pp. 5326–5334, Dec. 2016, doi: 10.1109/TAP.2016.2617376.

[42] O. M. Bucci, "Computational complexity in the solution of large antenna and scattering problems," *Radio Sci.*, vol. 40, no. 6, pp. 1–9, 2005, doi: 10.1029/2004RS003196.

[43] A. C. Newell, "Error analysis techniques for planar near-field measurements," *IEEE Trans. Antennas Propag.*, vol. 36, no. 6, pp. 754–768, Jun. 1988, doi: 10.1109/8.1177.

[44] F. Ferrara, C. Gennarelli, R. Guerriero, G. Riccio, and C. Savarese, "An efficient near-field to far-field transformation using the planar wide-mesh scanning," *J. Electromagn. Waves Appl.*, vol. 21, no. 3, pp. 341–357, 2007, doi: 10.1163/156939307779367404.

[45] L. I. Williams, Y. Rahmat-Samii, and R. G. Yaccarino, "The bi-polar planar near-field measurement technique, part i: Implementation and measurement comparisons," *IEEE Trans. Antennas Propag.*, vol. 42, no. 2, pp. 184–195, Feb. 1994, doi: 10.1109/8.277212.

[46] R. Yaccarino, Y. Rahmat-Samii, and L. Williams, "The bi-polar planar near-field measurement technique, part ii: Near-field to far-field transformation and holographic imaging methods," *IEEE Trans. Antennas Propag.*, vol. 42, no. 2, pp. 196–204, Feb. 1994, doi: 10.1109/8.277213.

[47] O. Bucci, C. Gennarelli, G. Riccio, and C. Savarese, "Probe compensated NF-FF transformation with helicoidal scanning," *J. Electromagn. Waves Appl.*, vol. 14, no. 4, pp. 531–549, 2000, doi: 10.1080/09205071.2000.9756677.

[48] O. Bucci, F. D'Agostino, C. Gennarelli, G. Riccio, and C. Savarese, "Probe compensated far-field reconstruction by near-field planar spiral scanning," *IEE Proc.-Microw., Antennas Propag.*, vol. 149, no. 2, pp. 119–123, 2002, doi: 10.1049/ip-map:20020265.

[49] O. Bucci, G. D'Elia, and M. Migliore, "Advanced field interpolation from plane-polar samples: Experimental verification," *IEEE Trans. Antennas Propag.*, vol. 46, no. 2, pp. 204–210, Feb. 1998, doi: 10.1109/8.660964.

[50] F. Musters, R. Coesoij, M. Migliore, F. Schettino, and M. Spirito, "The antenna dome real-time distributed antenna pattern characterization system," in *Proc. 97th ARFTG Microw. Meas. Conf. (ARFTG)*, Piscataway, NJ, USA: IEEE Press , 2021, pp. 1–5, doi: 10.1109/ARFTG52261.2021.9640079.

[51] C. Gennarelli, F. Ferrara, R. Guerriero, and F. D'Agostino, *Non-Redundant Near-Field to Far-Field Transformation Techniques*. Institution of Engineering and Technology, Stevenage, U.K., 2023.

[52] O. M. Bucci, C. Gennarelli, G. Riccio, and C. Savarese, "Electromagnetic fields interpolation from nonuniform samples over spherical and cylindrical surfaces," *IEE Proc.-Microwa., Antennas Propag.*, vol. 141, no. 2, pp. 77–84, 1994, doi: 10.1049/ip-map:19949838.

[53] O. Bucci, G. D'Elia, and M. Migliore, "A new strategy to reduce the truncation error in near-field/far-field transformations," *Radio Sci.*, vol. 35, no. 1, pp. 3–17, 2000, doi: 10.1029/1999RS900073.

[54] J. Bolomey, O. M. Bucci, L. Casavola, G. D'Elia, M. D. Migliore, and A. Ziyyat, "Reduction of truncation error in near-field measurements of antennas of base-station mobile communication systems," *IEEE Trans. Antennas Propag.*, vol. 52, no. 2, pp. 593–602, Feb. 2004, doi: 10.1109/TAP.2004.823999.

[55] O. M. Bucci and M. D. Migliore, "A new method for avoiding the truncation error in near-field antennas measurements," *IEEE Trans. Antennas Propag.*, vol. 54, no. 10, pp. 2940–2952, Oct. 2006, doi: 10.1109/TAP.2006.882151.

[56] O. M. Bucci, G. D'Elia, and M. D. Migliore, "An effective near-field far-field transformation technique from truncated and inaccurate amplitude-only data," *IEEE Trans. Antennas Propag.*, vol. 47, no. 9, pp. 1377–1385, Sep. 1999, doi: 10.1109/8.793317.

[57] O. M. Bucci, G. D'Elia, and D. Migliore, "Optimal time-domain field interpolation from plane-polar samples," *IEEE Trans. Antennas Propag.*, vol. 45, no. 6, pp. 989–994, Jun. 1997, doi: 10.1109/8.585746.

[58] O. M. Bucci, G. D'Elia, and M. D. Migliore, "Near-field far-field transformation in time domain from optimal plane-polar samples," *IEEE Trans. Antennas Propag.*, vol. 46, no. 7, pp. 1084–1088, Jul. 1998, doi: 10.1109/8.704812.

[59] O. M. Bucci and M. D. Migliore, "Effective estimation of 2-D monostatic radar cross sections from near-field measurements," *IEEE Trans. Antennas Propag.*, vol. 54, no. 2, pp. 750–752, Feb. 2006, doi: 10.1109/TAP.2005.863154.

[60] M. D. Migliore, "On the sampling of the electromagnetic field radiated by sparse sources," *IEEE Trans. Antennas Propag.*, vol. 63, no. 2, pp. 553–564, Feb. 2015, doi: 10.1109/TAP.2014.2379911.

[61] O. Bucci, G. D'Elia, and M. D. Migliore, "A general and effective clutter filtering strategy in near-field antenna measurements," *IEE Proc.-Microw., Antennas Propag.*, vol. 151, no. 3, pp. 227–235, 2004, doi: 10.1049/ip-map:20040267.

[62] T. Isernia, O. Bucci, and N. Fiorentino, "Shaped beam antenna synthesis problems: Feasibility criteria and new strategies," *J. Electromagn. Waves Appl.*, vol. 12, no. 1, pp. 103–138, 1998, doi: 10.1163/156939398X00098.

[63] O. M. Bucci, G. D'Elia, G. Mazzarella, and G. Panariello, "Antenna pattern synthesis: A new general approach," *Proc. IEEE*, vol. 82, no. 3, pp. 358–371, Mar. 1994, doi: 10.1109/5.272140.

[64] L. Gubin, B. T. Polyak, and E. Raik, "The method of projections for finding the common point of convex sets," *USSR Comput. Math. Math. Phys.*, vol. 7, no. 6, pp. 1–24, 1967, doi: 10.1016/0041-5553(67)90113-9.

[65] O. M. Bucci, T. Isernia, and A. F. Morabito, "Optimal synthesis of circularly symmetric shaped beams," *IEEE Trans. Antennas Propag.*, vol. 62, no. 4, pp. 1954–1964, Apr. 2014, doi: 10.1109/TAP.2014.2302842.

[66] G. Toso, C. Mangenot, and A. Roederer, "Sparse and thinned arrays for multiple beam satellite applications," in *Proc. 2nd Eur. Conf. Antennas Propag. (EuCAP)*, IET, 2007, pp. 1–4.

[67] O. M. Bucci, M. D'Urso, T. Isernia, P. Angeletti, and G. Toso, "Deterministic synthesis of uniform amplitude sparse arrays via new density taper techniques," *IEEE Trans. Antennas Propag.*, vol. 58, no. 6, pp. 1949–1958, Jun. 2010, doi: 10.1109/TAP.2010.2046831.

[68] O. M. Bucci and S. Perna, "A deterministic two dimensional density taper approach for fast design of uniform amplitude pencil beams arrays," *IEEE Trans. Antennas Propag.*, vol. 59, no. 8, pp. 2852–2861, Aug. 2011, doi: 10.1109/TAP.2011.2158783.

[69] O. M. Bucci, M. D. Migliore, G. Panariello, and D. Pinchera, "Plane-wave generators: Design guidelines, achievable performances and effective synthesis," *IEEE Trans. Antennas Propag.*, vol. 61, no. 4, pp. 2005–2018, Apr. 2013, doi: 10.1109/TAP.2012.2233453.

[70] A. J. Fenn, *Adaptive Phased Array Thermotherapy for Cancer*. Norwood, MA, USA: Artech House, 2009.

[71] O. Bucci and T. Isernia, "Electromagnetic inverse scattering: Retrievable information and measurement strategies," *Radio Sci.*, vol. 32, no. 6, pp. 2123–2137, 1997, doi: 10.1029/97RS01826.

[72] G. Leone, R. Persico, and R. Pierri, "Inverse scattering under the distorted born approximation for cylindrical geometries," *J. Opt. Soc. Am. A*, vol. 16, no. 7, pp. 1779–1787, 1999, doi: 10.1364/JOSAA.16.001779.

[73] R. Pierri and G. Leone, "Inverse scattering of dielectric cylinders by a second-order born approximation," *IEEE Trans. Geosci. Remote Sens.*, vol. 37, no. 1, pp. 374–382, Jan. 1999, doi: 10.1109/36.739072.

[74] A. S. Poon, R. W. Brodersen, and D. N. Tse, "Degrees of freedom in multiple-antenna channels: A signal space approach," *IEEE Trans. Inf. Theory*, vol. 51, no. 2, pp. 523–536, Feb. 2005, doi: 10.1109/TIT.2004.840892.

[75] F. K. Gruber and E. A. Marengo, "New aspects of electromagnetic information theory for wireless and antenna systems," *IEEE Trans. Antennas Propag.*, vol. 56, no. 11, pp. 3470–3484, Nov. 2008, doi: 10.1109/TAP.2008.2005468.

[76] R. Janaswamy, "On the EM degrees of freedom in scattering environments," *IEEE Trans. Antennas Propag.*, vol. 59, no. 10, pp. 3872–3881, Oct. 2011, doi: 10.1109/TAP.2011.2163776.

[77] M. D. Migliore, "Horse (electromagnetics) is more important than horseman (information) for wireless transmission," *IEEE Trans. Antennas Propag.*, vol. 67, no. 4, pp. 2046–2055, Apr. 2019, doi: 10.1109/TAP.2018.2889158.

[78] M. Franceschetti, M. D. Migliore, and P. Minero, "The capacity of wireless networks: Information-theoretic and physical limits," *IEEE Trans. Inf. Theory*, vol. 55, no. 8, pp. 3413–3424, Aug. 2009, doi: 10.1109/TIT.2009.2023705.

[79] R. Somaraju and J. Trumpf, "Degrees of freedom of a communication channel: Using DOF singular values," *IEEE Trans. Inf. Theory*, vol. 56, no. 4, pp. 1560–1573, Apr. 2010, doi: 10.1109/TIT.2010.2040895.

[80] M. Di Renzo and M. D. Migliore, "Electromagnetic signal and information theory," *IEEE BITS Inf. Theory Mag.*, early access, Jan. 29, 2024, doi: 10.1109/MBITS.2024.3359523.

[81] M. Jian et al., "Reconfigurable intelligent surfaces for wireless communications: Overview of hardware designs, channel models, and estimation techniques," *Intell. Converged Netw.*, vol. 3, no. 1, pp. 1–32, 2022, doi: 10.23919/ICN.2022.0005.

[82] M. D. Migliore, D. Pinchera, M. Lucido, F. Schettino, and G. Panariello, "An electromagnetic analysis of noise-based intrinsically secure communication in wireless systems," *Electronics*, vol. 7, no. 7, 2018, Art. no. 113, doi: 10.3390/electronics7070113.